Atlas of Sonographic Anatomy of the Hand and Wrist

Afarine Madani, MD, PhD[a], Viviane Créteur, MD[b],*, Stefano Bianchi, MD[c]

KEYWORDS

• US • Hand • Wrist • Atlas • Normal anatomy

KEY POINTS

- Understanding US indications.
- Understanding US technique.
- Learning normal US appearance of wrist, hand, and fingers.

INTRODUCTION

X-rays have been traditionally used for the evaluation of bones, joints, and soft tissue calcifications.[1] In recent years, the role of musculoskeletal ultrasonography (US), particularly in the wrist and hand, has expanded dramatically for both diagnostic and interventional purposes.[2–4] Three main conditions are essential to perform an optimal US examination of the wrist and hand.

The first condition is equipment quality and standardized examination technique. Optimal equipment includes high-frequency linear array transducers ranging from 10 to 15 MHz, with an adapted size and shape of the probe, like a hockey-stick probe; Doppler imaging; compound imaging; extended field-of-view imaging; steering-based imaging; 3-dimensional imaging; elastography; contrast media; and DICOM capacities for static and dynamic recording.[5] Standardization of US examination technique involves examination first on the short axis and then on the long axis plane, performing dynamic evaluation, and correct focusing.

The second condition is appropriate US indications, pertinent clinical information, and patient's history.

The third condition is accurate interpretation of the images and correlation of the US findings with clinical data.

US may be applied to the bone as an adjunct to x-rays in selected cases because it can detect superficial cortical outgrowths or ingrowths.[6–9]

The US appearance of muscles and tendons is well known.[10,11] Normal skeletal muscles appear relatively hypoechoic with hyperechoic linear strands or dots, whereas normal tendons and ligaments appear highly hyperechoic because of their tight and compact fibrillar pattern. Tendons, like ligaments, are subject to anisotropy.[12,13]

In transverse view, nerves appear as round/ovoid structures composed of hypoechoic spots, corresponding to fascicles, embedded in a hyperechoic background, corresponding to the interfascicular epineurium.[11] In longitudinal view, they appear as fascicular structures composed of hypoechoic parallel linear areas separated by hyperechoic bands.[14,15]

[a] Service de Radiologie, Department of Radiology, CUB Hôpital Erasme, Université Libre de Bruxelles, 808, Route de Lennik, Brussels 1070, Belgium; [b] Department of Radiology, CUB Hôpital Erasme, Université Libre de Bruxelles, 808, Route de Lennik, Brussels 1070, Belgium; [c] CIM SA, Cabinet d'imagerie médicale, 40a route de Malagnou, Geneva 1208, Switzerland
* Corresponding author. 40, rue Haut du village, Sautour 5600, Belgium.
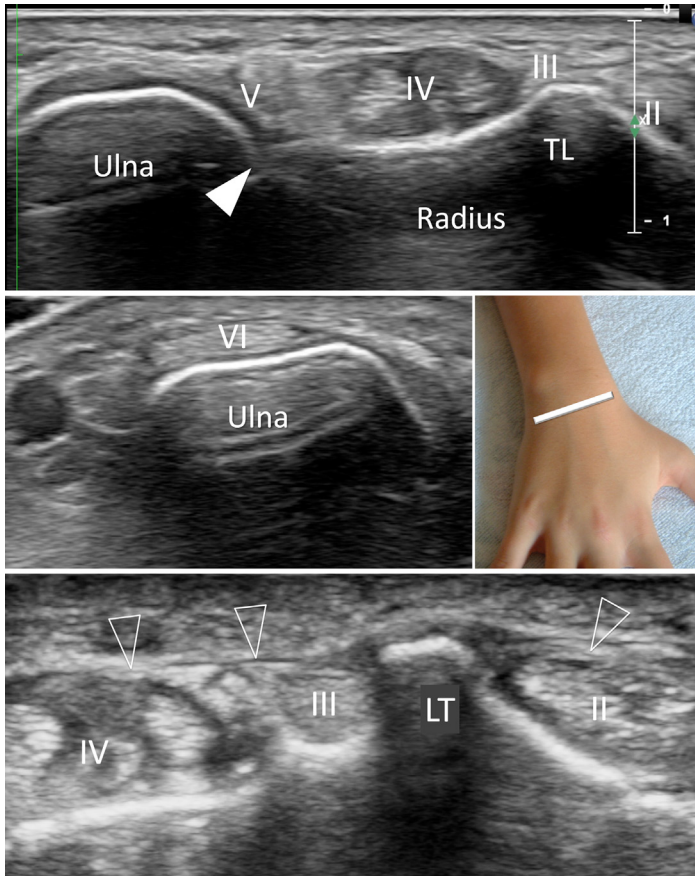E-mail address: viviane.creteur@gmail.com

Fig. 1. At the dorsal wrist, 3 key structures are noticeable on an axial view: the dorsal tubercle of the radius, the extensor retinaculum (*open arrowheads*), and the distal radioulnar joint (*arrowhead*). The extensor retinaculum divides the dorsal wrist into 6 distinct compartments (I–VI). LT, lunotriquetral ligament; TL, Lister tubercle.
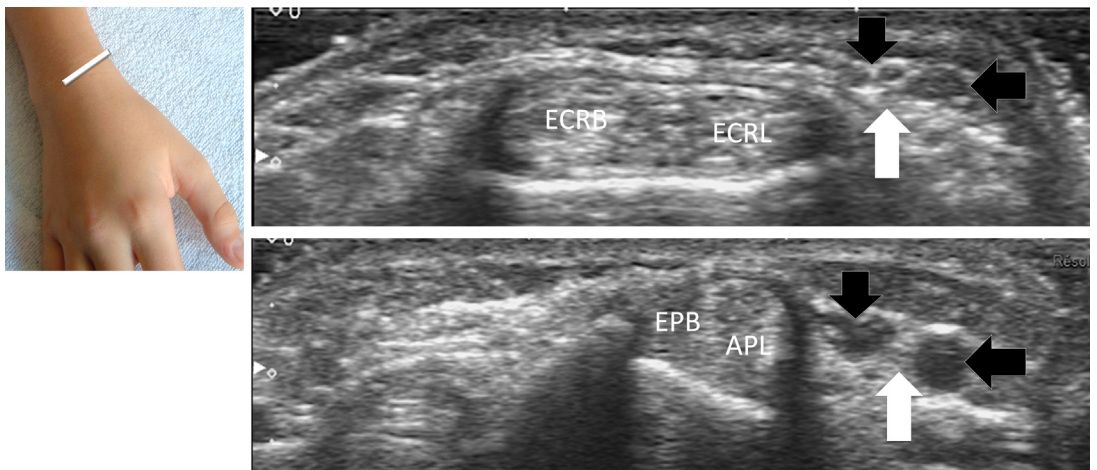

Fig. 2. On the radial side of the Lister tubercle, compartment I contains APL and EPB tendons, and compartment II contains ECRB and ECRL tendons. The cutaneous branch of the radial nerve (*white arrows*) and the cephalic vein (*black arrows*) are visible near these tendons. Excessive pressure of the probe may avoid visualization of small structures, such as superficial veins and nerves. APL, abductor pollicis longus; ECRB, extensor carpi radialis brevis; ECRL, extensor carpi radialis longus; EPB, extensor pollicis brevis.
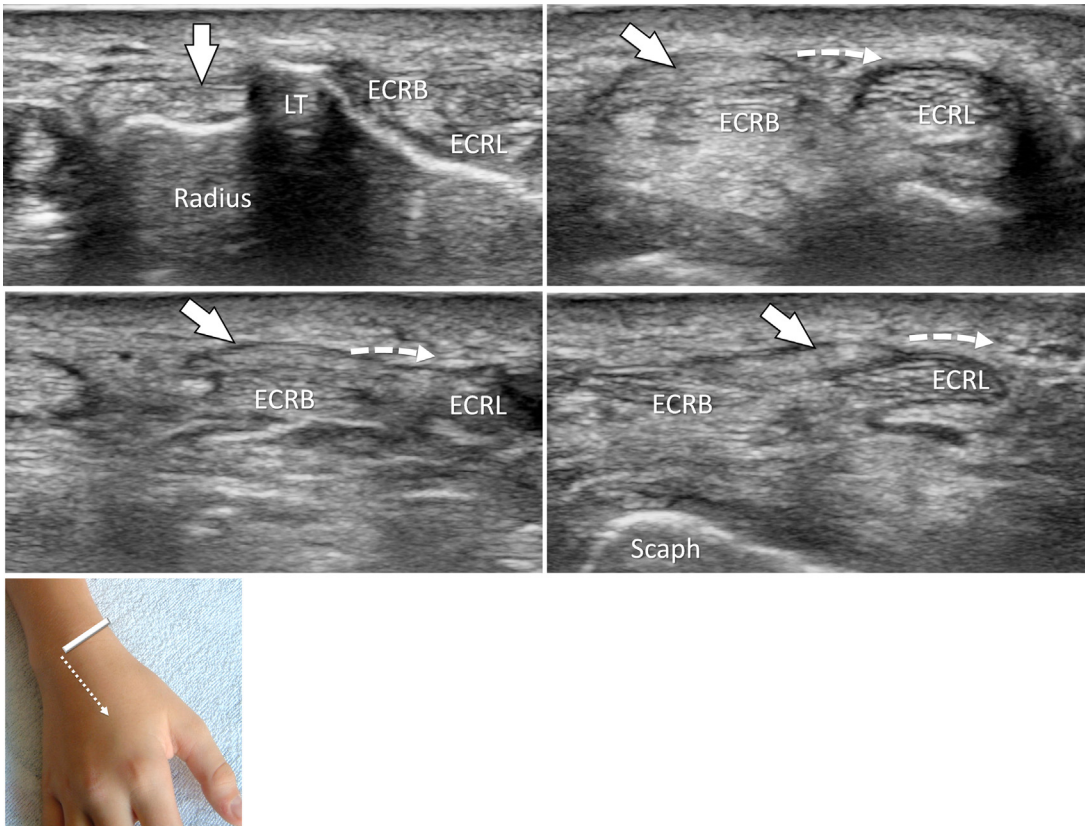
Fig. 3. When using the "elevator technique" from the Lister tubercle toward the scaphoid bone, axial US images display the proximal intersection of the radial tendons. The EPL tendon (compartment III, *white arrow*) crosses (*dotted curved arrow*) the ECRB and ECRL tendons (compartment II). This peculiar anatomic situation may lead to the so-called intersection syndrome, which is usually secondary to occupational repetitive flexion and extension of the wrist. This condition may be easily confused with De Quervain disease. Dotted arrow on artwork illustrates the axial progression of the probe from proximal to distal wrist. EPL, extensor pollicis longus; ECRB, extensor carpi radialis brevis; ECRL, extensor carpi radialis longus; Scaph, scaphoid.
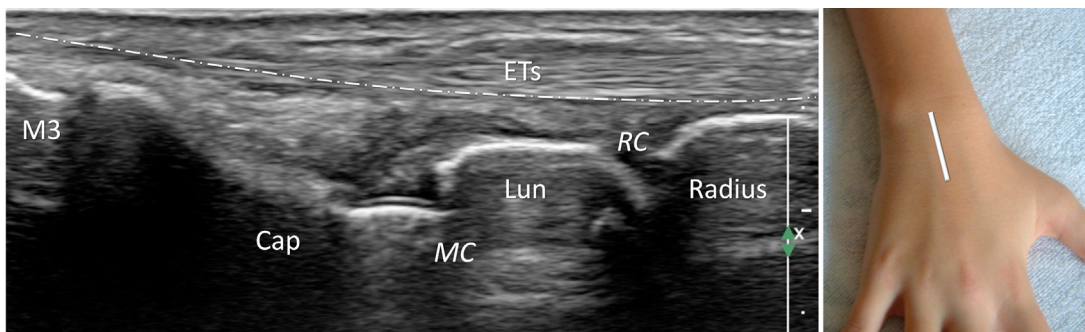

Fig. 4. In the longitudinal view performed at the level of the third metacarpal, carpal bone outlines are hyperechoic, regular, and relatively straight (*straight dotted line*). The RC and MC joints are visible. This view allows quick detection of synovial thickening or fluid. Cap, capitate; ETs, extensor tendons; Lun, lunate; MC, midcarpal joint; RC, radiocarpal joint.
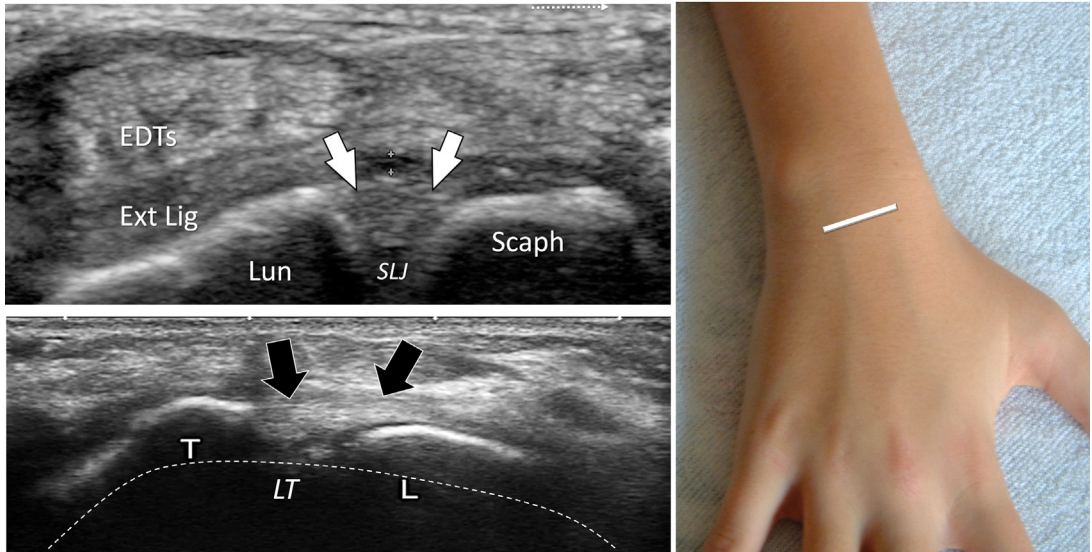
Fig. 5. Extrinsic ligaments connect the radius, ulna, and metacarpals with the carpal bones. These ligaments are partially visible underneath the extensor digitorum tendons, close to the bones. Intrinsic ligaments connect the carpal bones to one another. The most relevant ligaments seen on US are the SL (*white arrows*) and LT (*black arrows*) ligaments. These ligaments are better visualized on axial views. Observe that the carpal bones appear convex (*curved dotted line*) in the dorsal axial view but concave in the palmar axial view (see carpal tunnel, Fig. 13). EDTs, extensor digitorum communis tendons; Ext Lig, extrinsic ligament; L, Lu, lunate; SL, scapholunate ligament; SLJ, scapholunate joint; T, triquetrum.
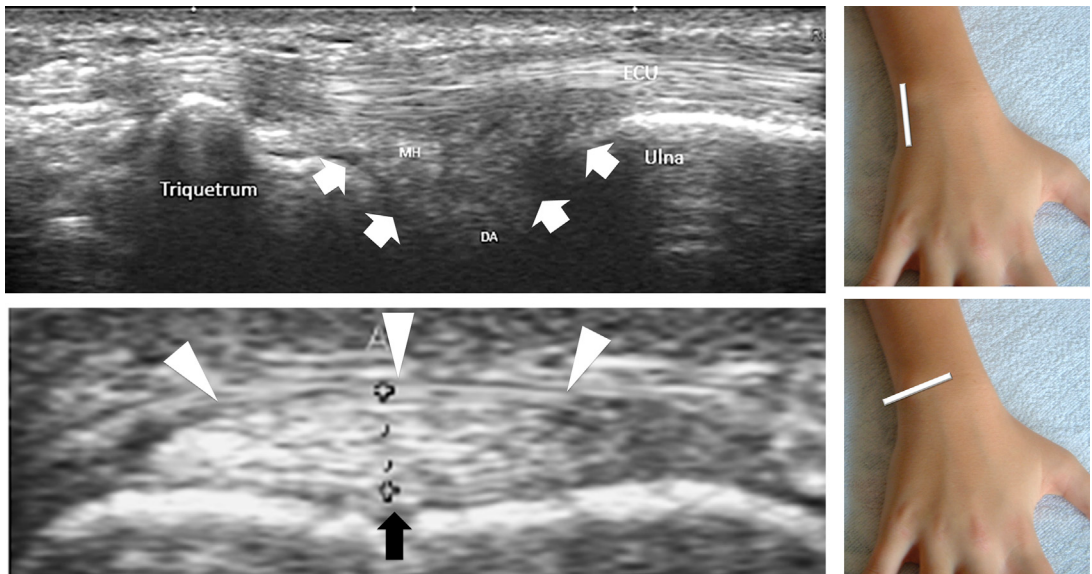

Fig. 6. At the ulnar side of the wrist, the triangular fibrocartilage complex is located between the ulnar styloid and distal radius (white arrows). The complex is composed of the triangular biconcave fibrocartilage, meniscus homologue, ulnar collateral ligament, radioulnar ligaments, and sheath (*arrowheads*) of the ECU (*black arrow*). Even with high-resolution transducers, US cannot distinguish the different components of the triangular fibrocartilage complex. Their accurate evaluation requires other modalities such as MRI or computed tomography with arthrography. DA, deep arterial arch; ECU, extensor carpi ulnaris; MH, meniscus homologue.
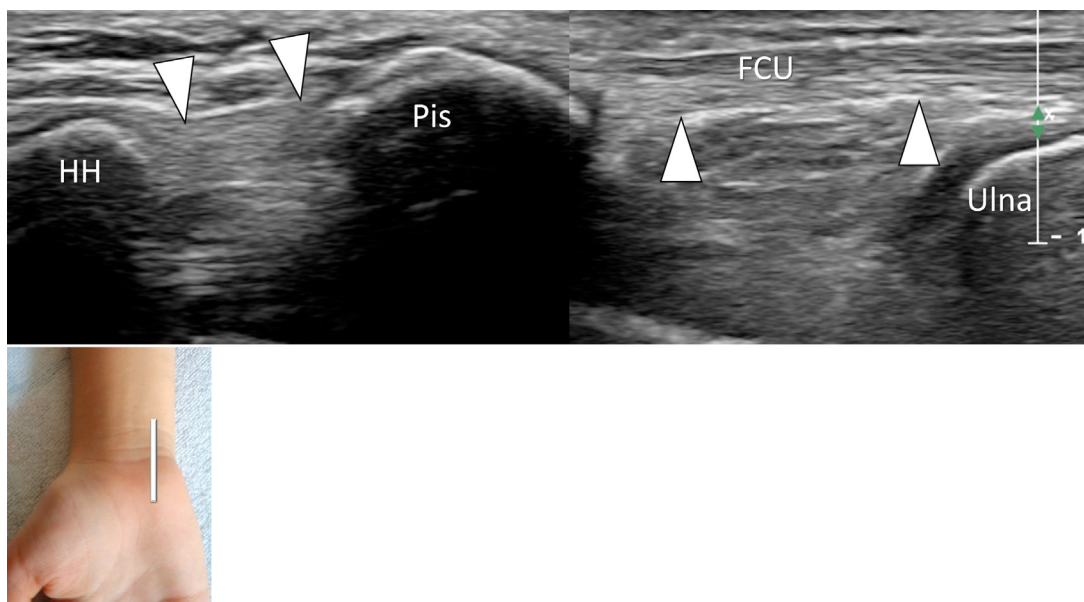
Fig. 7. Apart from the palmaris longus, the FCU (*arrowheads*) is the only wrist tendon without a synovial sheath. The FCU inserts into the pisiform. The pisohamate ligament is a prolongation of the FCU and serves as part of the origin of the ADM. ADM, adductor digiti minimi; FCU, flexor carpi ulnaris; HH, hamate hook; Pis, pisiform.

The US appearance of normal vessels has been documented. Compared with arteries, veins have thinner walls and larger lumens. In the wrist and hand, these vessels are relatively superficial, and their location may be easier to detect with color Doppler US.[16]

In this practical pictorial, we review the essentials of the US anatomy of the wrist and the hand.

Anatomic Structures Detected on Ultrasonography

Wrist: carpal joints, selected ligaments (scapholunate, lunotriquetral, and pisohamate ligaments), flexor and extensor tendons, retinacula, and neurovascular structures.[2–4,16]

Hand: muscles, joints, several ligaments (collateral metacarpophalangeal ligament of the thumb, collateral radial metacarpophalangeal ligament of the index, collateral ulnar metacarpophalangeal ligament of the fifth finger, and interphalangeal collateral ligaments), palmar plate, flexor and extensor tendons, palmar aponeurosis, annular pulleys, and neurovascular structures.[17–21]

Normal Ultrasonographic Anatomy of the Wrist and Hand

Although the position of the wrist and hand, as well as the location of the sonographer, may differ in the operating room of the surgeon than in the consultant room of the radiologist, the realization of US must be similar: beginning with axial views using the "elevator technique" and anatomic landmarks and followed by longitudinal images. Then, US images are obtained in different positions of the wrist and hand (such as flexion, extension, radial and ulnar deviation, pronation, supination, and active and passive movements), allowing dynamic evaluation of the region. US assessment of the wrist and hand should be complete, although extra attention could be paid to a special finding or a particular region of clinical interest.

To facilitate the interpretation of typical US images, the extensor (dorsal) and flexor (palmar) regions must be considered separately. Typically, the wrist must be examined first in the axial and longitudinal planes (dorsal followed by volar aspects), and then each finger must be examined
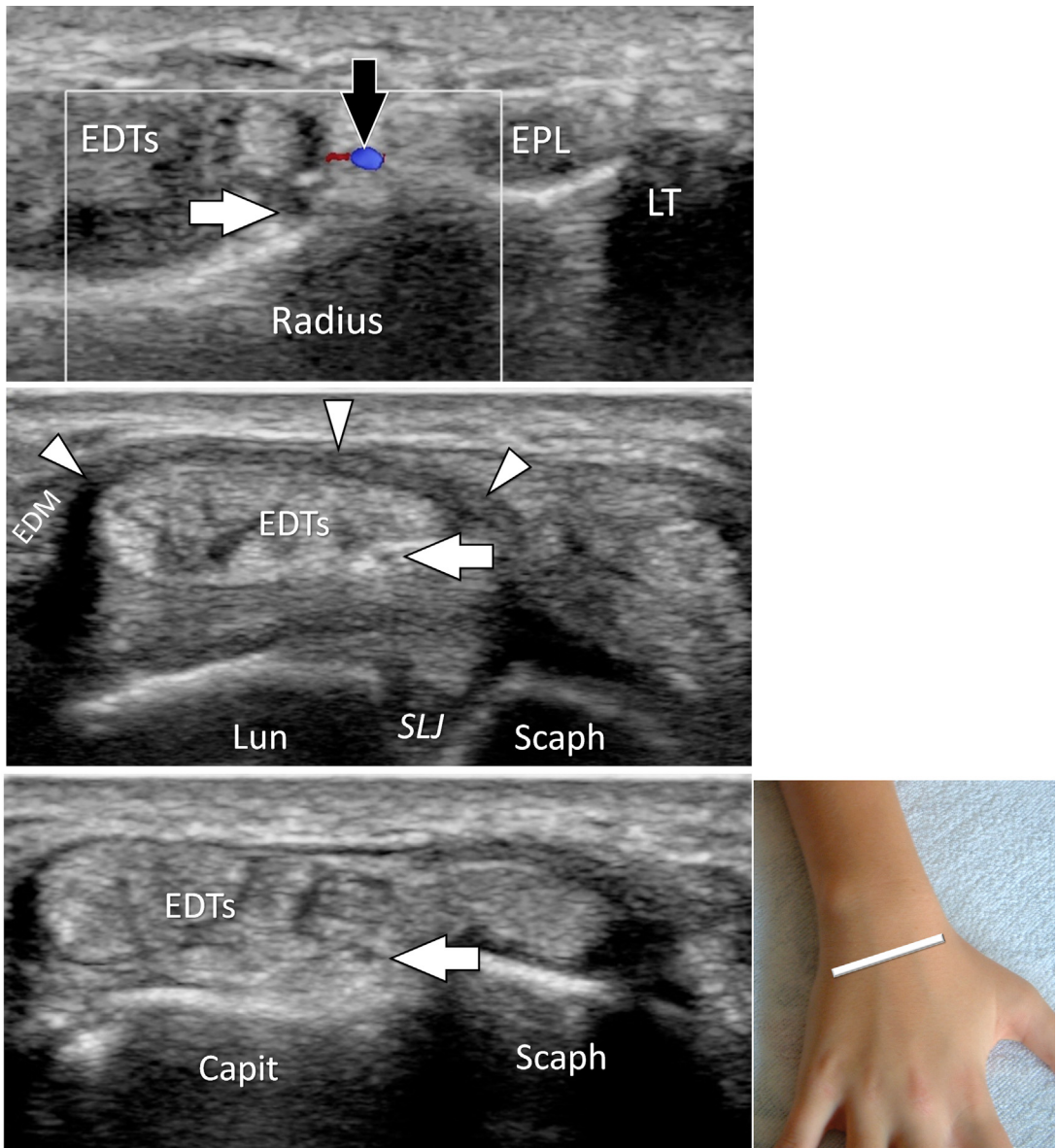
Fig. 8. At the ulnar side of the Lister tubercle, compartments III–V contain the EPL, EDTs, and EDM, respectively. The extensor retinaculum (*arrowheads*) surrounding the extensor tendons is clearly identified. The posterior interosseous nerve (*white arrow*) is deeply located and is accompanied by its artery (*black arrow*), which is easily identified using color Doppler US. This small nerve innervates only the dorsal wrist capsule and intra-articular structures. EDM, extensor digiti minimi; Capit, Capitate.
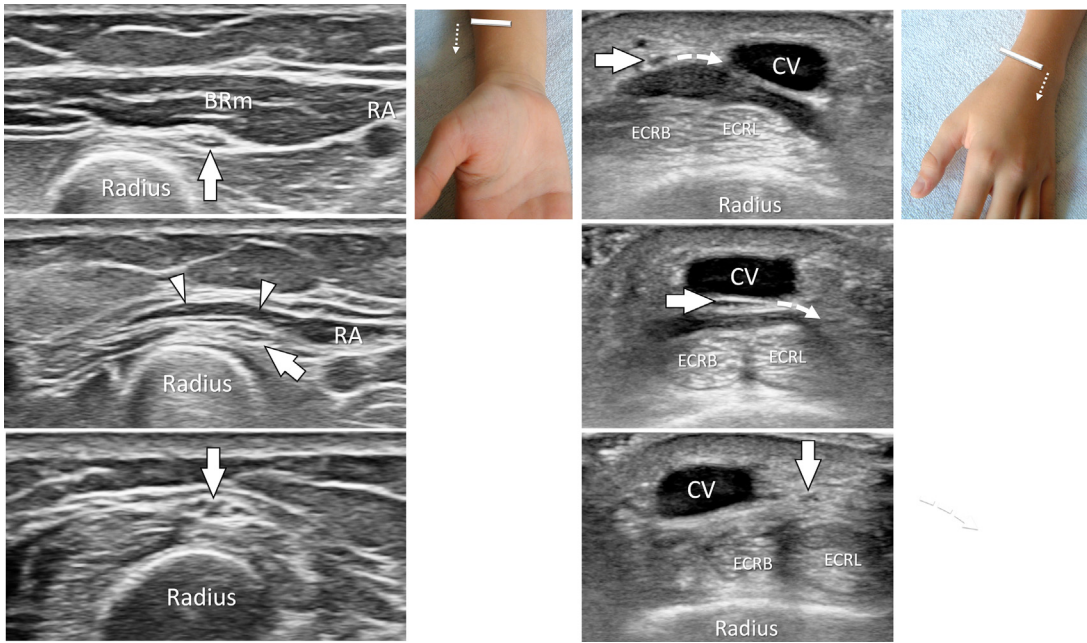
Fig. 9. The radial artery courses superficially with the radial nerve (*white arrow*) over the volar aspect of the distal radius, deep to the BRm and its tendon (*arrowheads*). The radial nerve then curves dorsally over the dorsal aspect of the wrist. At the distal radial aspect of the forearm, the superficial cutaneous branch of the radial nerve reaches the subcutaneous tissue between the ECRL and ECRB tendons, close to the cephalic vein (curved dotted arrow). BRm, brachioradialis muscle; CV, cephalic vein; RA, radial artery.
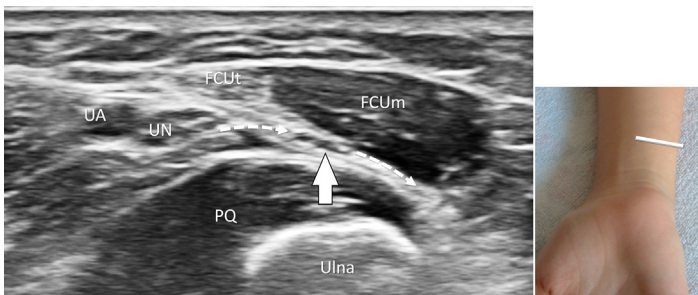

Fig. 10. In the distal volar forearm, the UN is located between the radial side of the FCUt and FCUm and the ulnar side of the UA. The UN gives off the dorsal cutaneous branch (*white arrow*) that runs between the FCUm superficially and the PQ deeply (*curved dotted arrow*). FCUm, flexor carpi ulnaris muscle; FCUt, flexor carpi ulnaris tendon; PQ, pronator quadratus; UA, ulnar artery; UN, ulnar nerve.
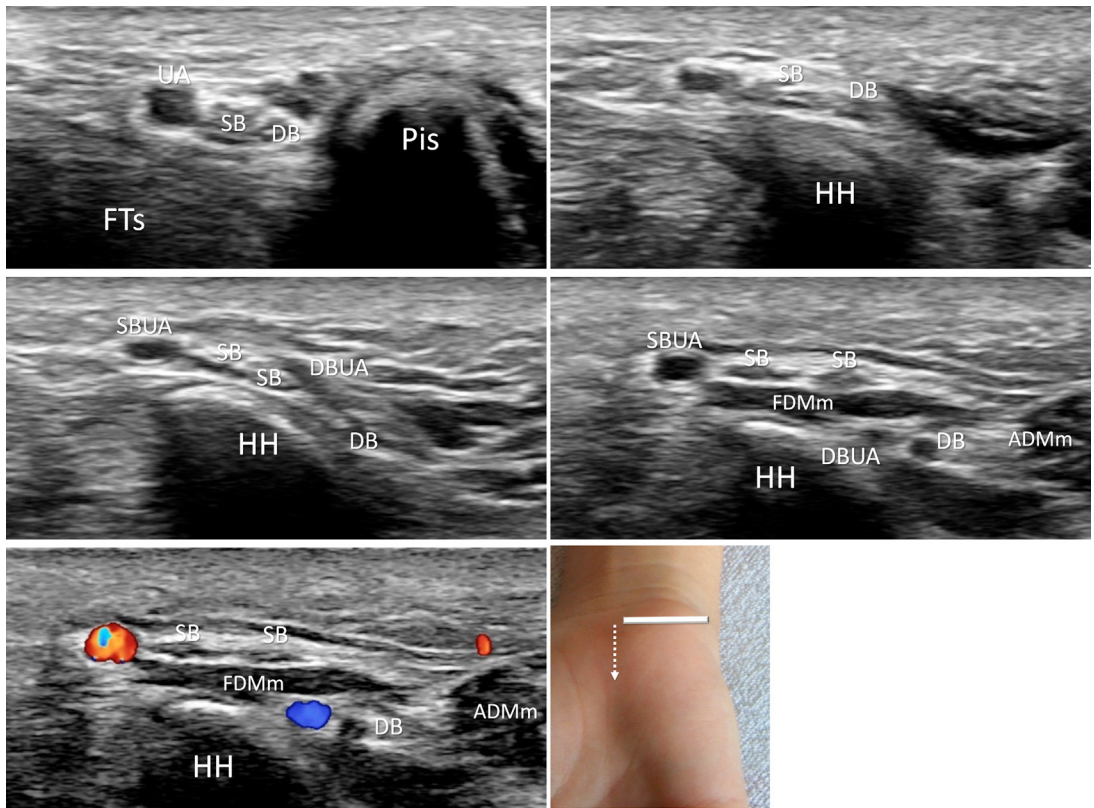
Fig. 11. The Guyon tunnel contains the UN medially and the UA laterally. The UN bifurcates within the tunnel, distal to the pisiform, in 2 terminal branches: SB and DB. The SB runs close to the UA, and the DB runs alongside to the hook of the hamate. Similarly, the UA splits into 2 branches—the SBUA and DBUA—following their respective nerves. ADMm, adductor digiti minimi muscle; DB, deep motor branch; DBUA, deep branch of ulnar artery; FDMm, flexor digiti minimi muscle; SB, sensory branch; SBUA, superficial branch of ulnar artery. Dotted arrow on artwork illustrates the axial progression of the probe from proximal to distal Guyon tunnel.
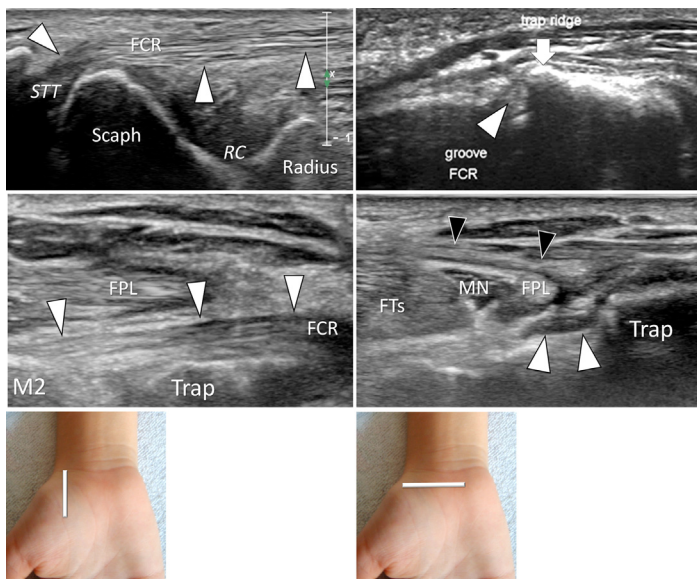

Fig. 12. The FCR (*white arrowheads*) courses in a separate fibrous tunnel made by an extension of the transverse carpal ligament (*black arrowheads*) inserted into the trapezial ridge (*arrow*). Then, the FCR reaches a groove situated on the ulnar side of the trapezium and inserts into the palmar aspect of the base of the second metacarpal. FCR, flexor carpi radialis; FPL, flexor pollicis longus; MN, median nerve; STT, scaphotrapezoid-trapezium joint; Trap, trapezium.
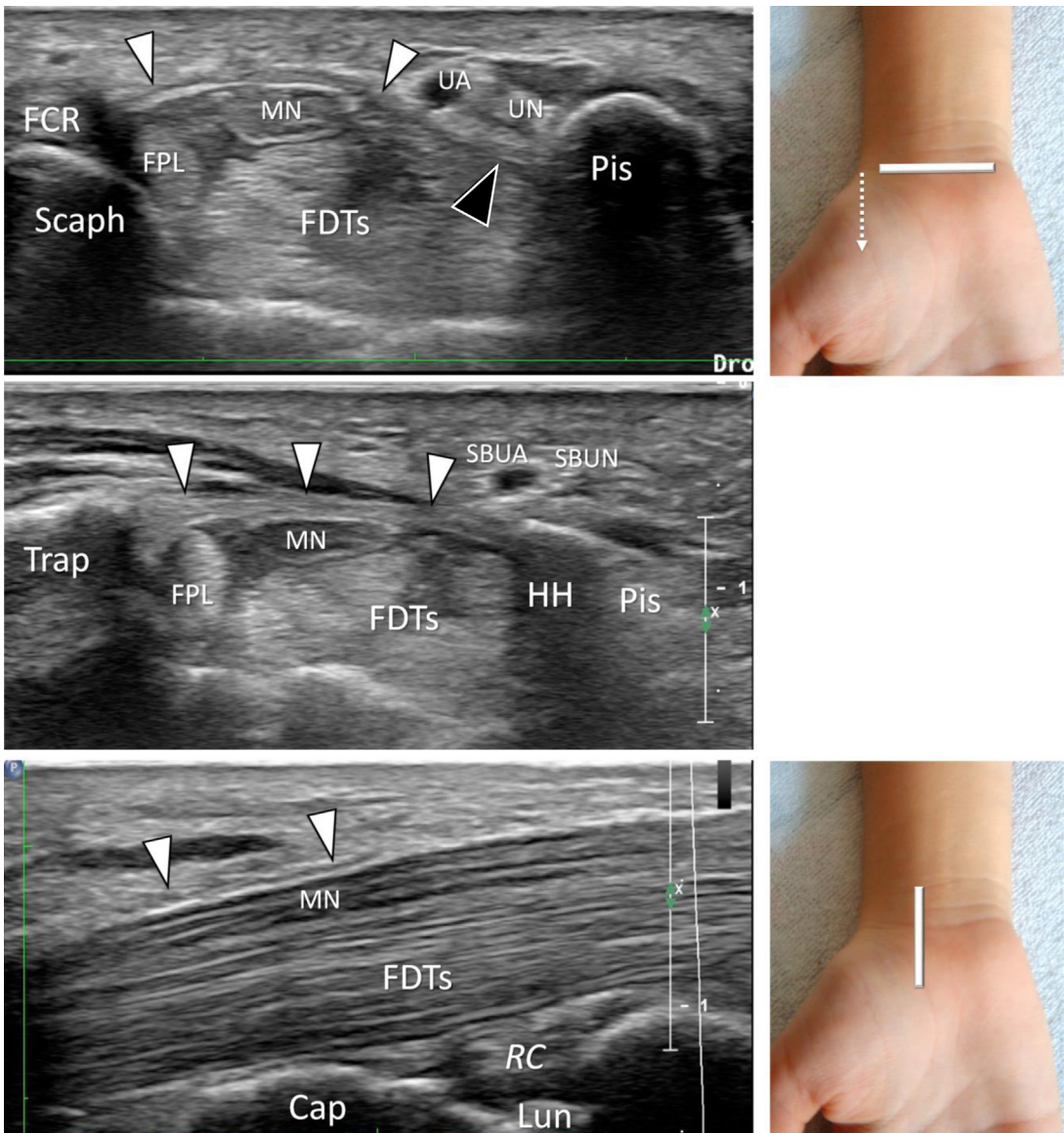
Fig. 13. The transverse carpal ligament (*white arrowheads*) forms the roof of the carpal tunnel and the floor of the Guyon tunnel (*black arrowhead*). Proximally, the carpal tunnel is delineated by the scaphoid at its radial side and the pisiform at its ulnar side. These bones appear as round hyperechoic structures with posterior acoustic shadows. Distally, the carpal tunnel is delineated by the trapezium at its radial side and the hook of the hamate at its ulnar side. The trapezium is characterized by its flat palmar surface, and the hook of the hamate is characterized by its short curvilinear shape. Because of the more central location of the hook of the hamate, the size of the distal tunnel is smaller than the proximal one. Within the carpal tunnel, the MN is located superficial to the FDTs and on the ulnar side of the FPL.FDTs, flexor digitorum tendons. Dotted arrow on artwork illustrates the axial progression of the probe from proximal to distal carpal.
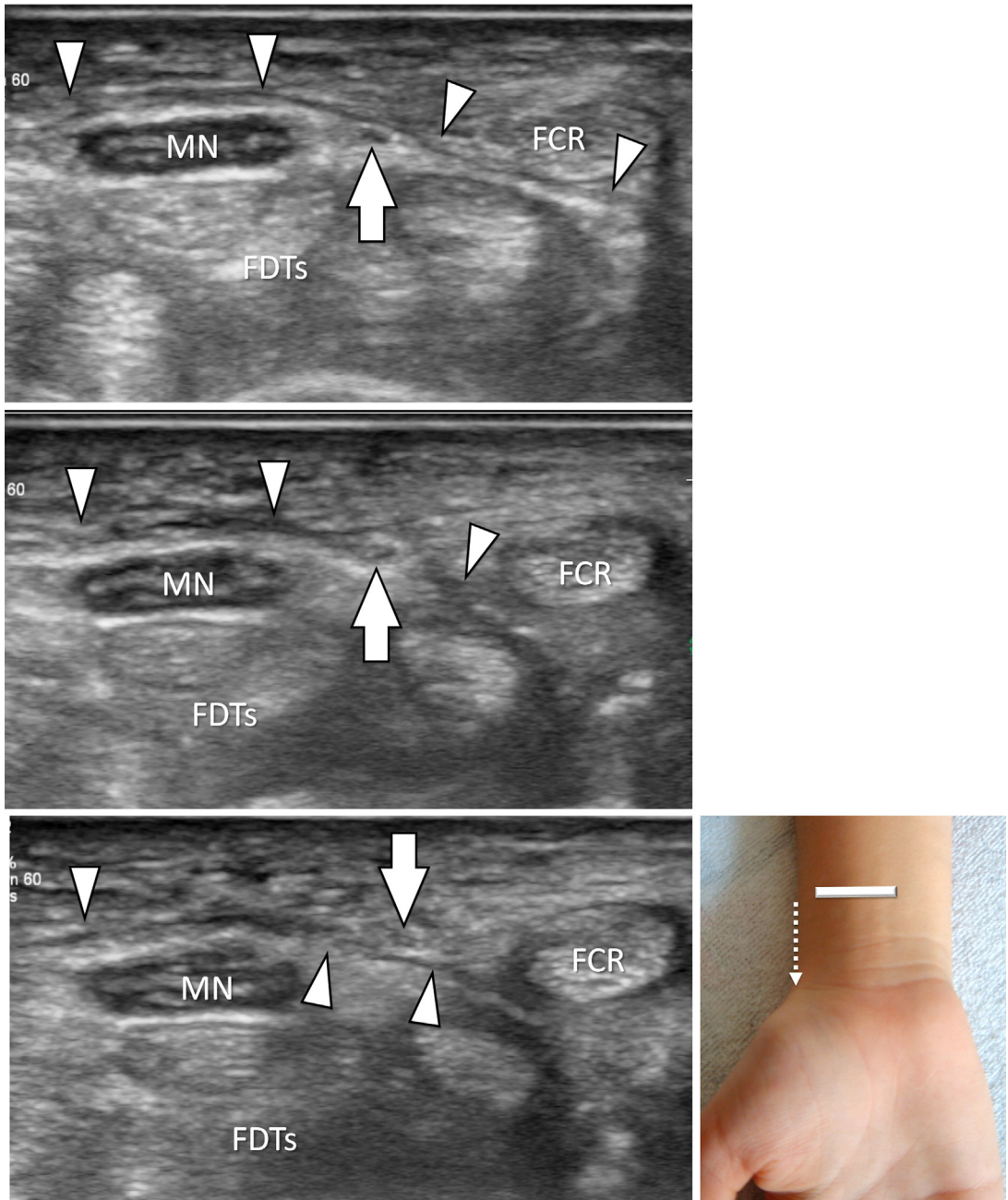
Fig. 14. The palmar cutaneous branch (*arrows*) of the MN arises from its palmar-radial quadrant, cranial to the proximal wrist crease. Then, it pierces the antebrachial fascia or the transverse carpal ligament (*arrowheads*), close to the FCR tendon. The dotted arrow indicates the progression of the probe from proximal to distal wrist.
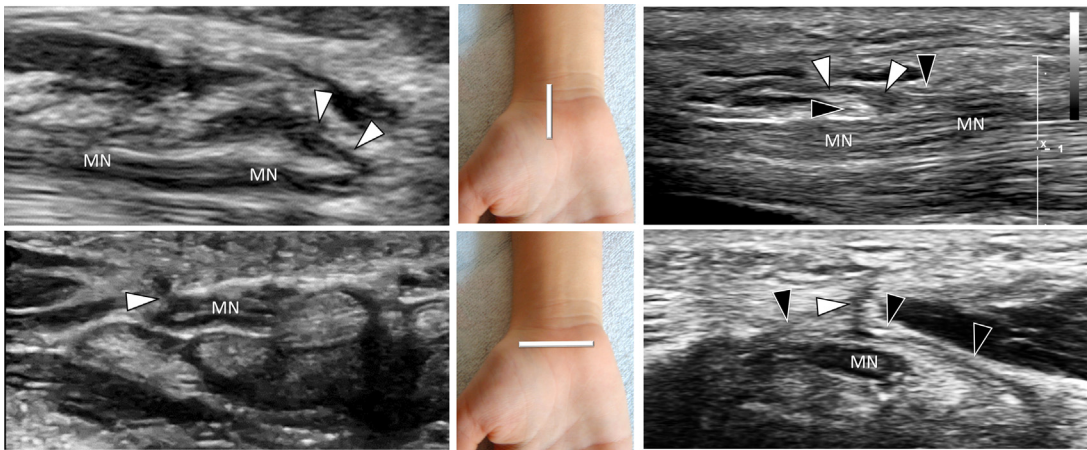
Fig. 15. Distal to the carpal tunnel, the MN gives off the thenar motor branch (*white arrowheads*). The classic extraligamentous course of the thenar branch is illustrated on the left US images. The transligamentous course of the thenar branch (*black arrowheads*), illustrated on the right US images, is seen in less than 4% of the population.
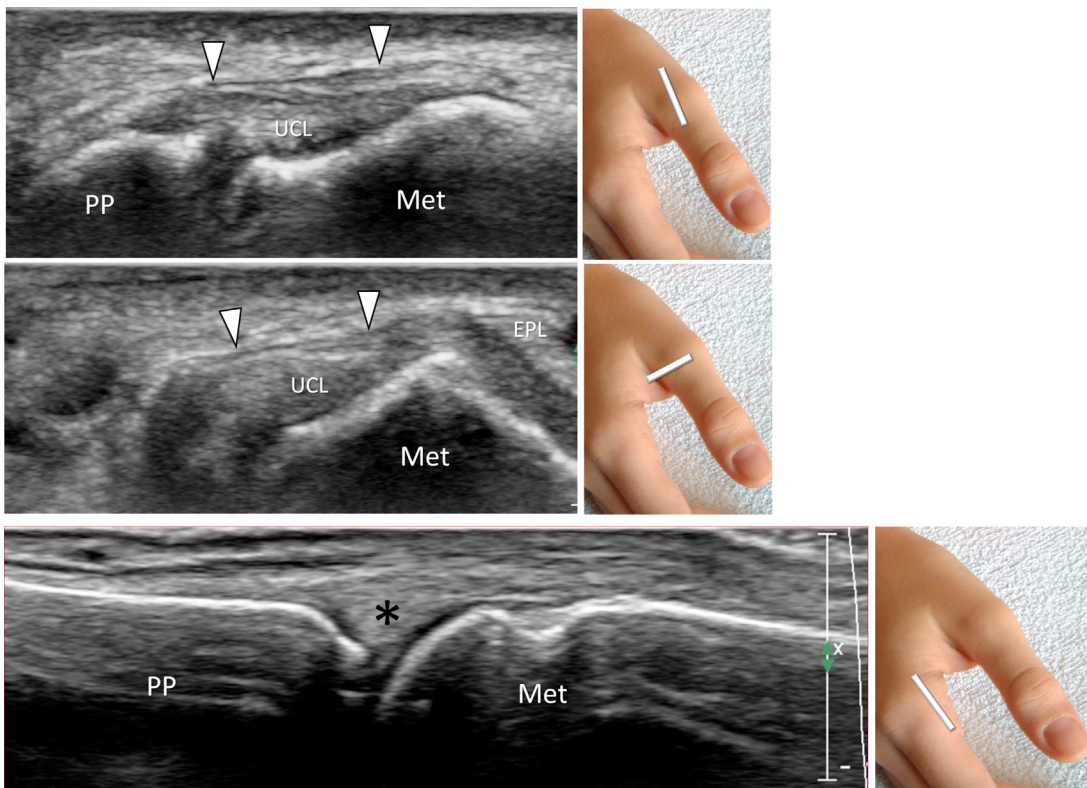

Fig. 16. Normal collateral ligaments of metacarpophalangeal joints may be easily seen on US only at the level of the thumb, the radial aspect of the second metacarpophalangeal joint, and the ulnar aspect of the fifth metacarpophalangeal joint. The ulnar collateral ligament (UCL) of the metacarpophalangeal joint of the thumb appears as a hyperechoic structure joining the first metacarpal to the proximal phalanx. Superficial to this ligament, the adductor pollicis muscle aponeurosis is visualized (*white arrowheads*). The radial collateral ligament of the second finger is illustrated as a thick hyperechoic structure (*asterisk*) close to the bone. Met, metacarpal; PP, proximal phalanx.
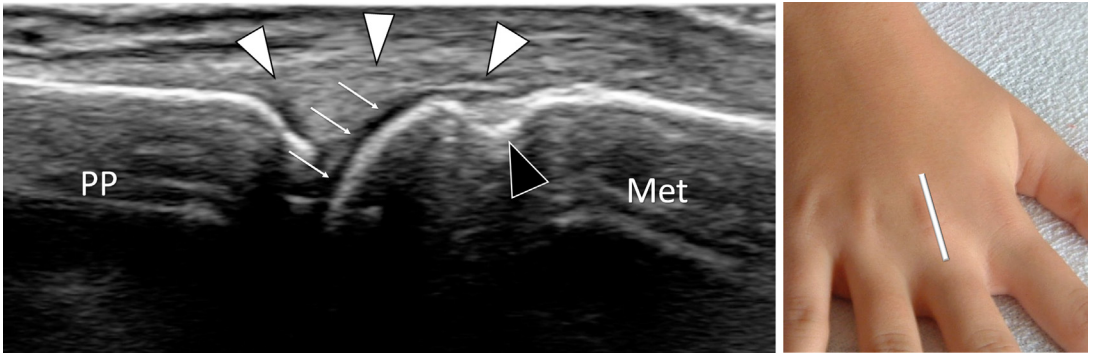
Fig. 17. In a longitudinal US view of the dorsal hand, the normal dorsal metacarpal notch (*black arrowhead*), measuring 0.7 to 2.2 mm, should not be confused with an erosion. The dorsal metacarpal synovial recess thickness (*white arrowheads*) should not exceed 2.2 mm. Fine hypoechoic cartilage covers the metacarpal head (*small arrows*).
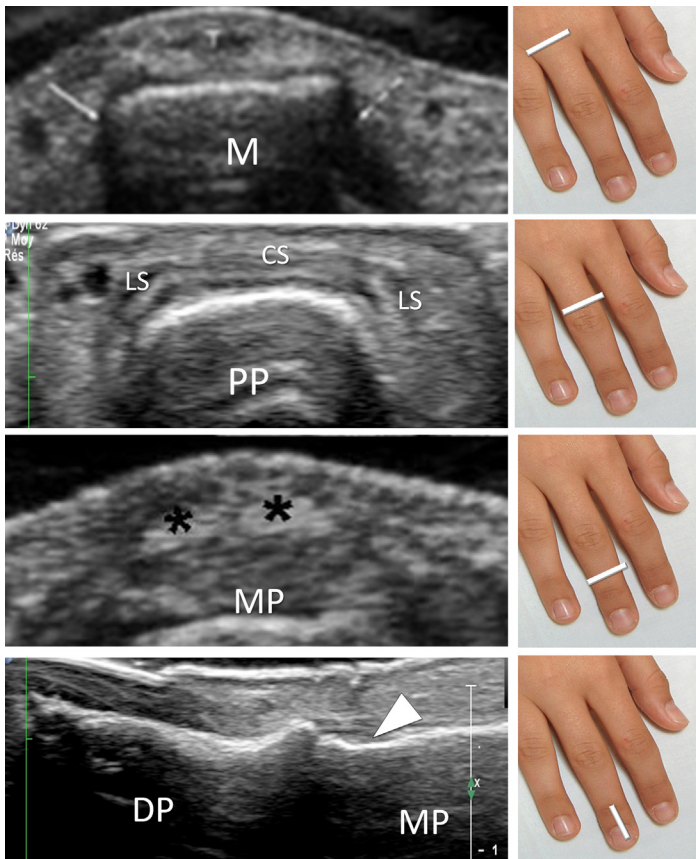

Fig. 18. Over the dorsal hand, the 4 tendons of the extensor digitorum muscle pass over the dorsal aspect of the metacarpal bones to reach the respective fingers. At the level of the metacarpal, the extensor tendon is covered by the sagittal band (*arrowhead*). At the level of the proximal phalanx, the extensor tendon divides into a central slip (CS) and 2 lateral slips (LSs). The CS inserts into the base of the middle phalanx, whereas the LSs (*asterisk*) fuse at the level of the MP to insert into the base of the distal phalanx. DP, distal phalanx; MP, middle phalanx.
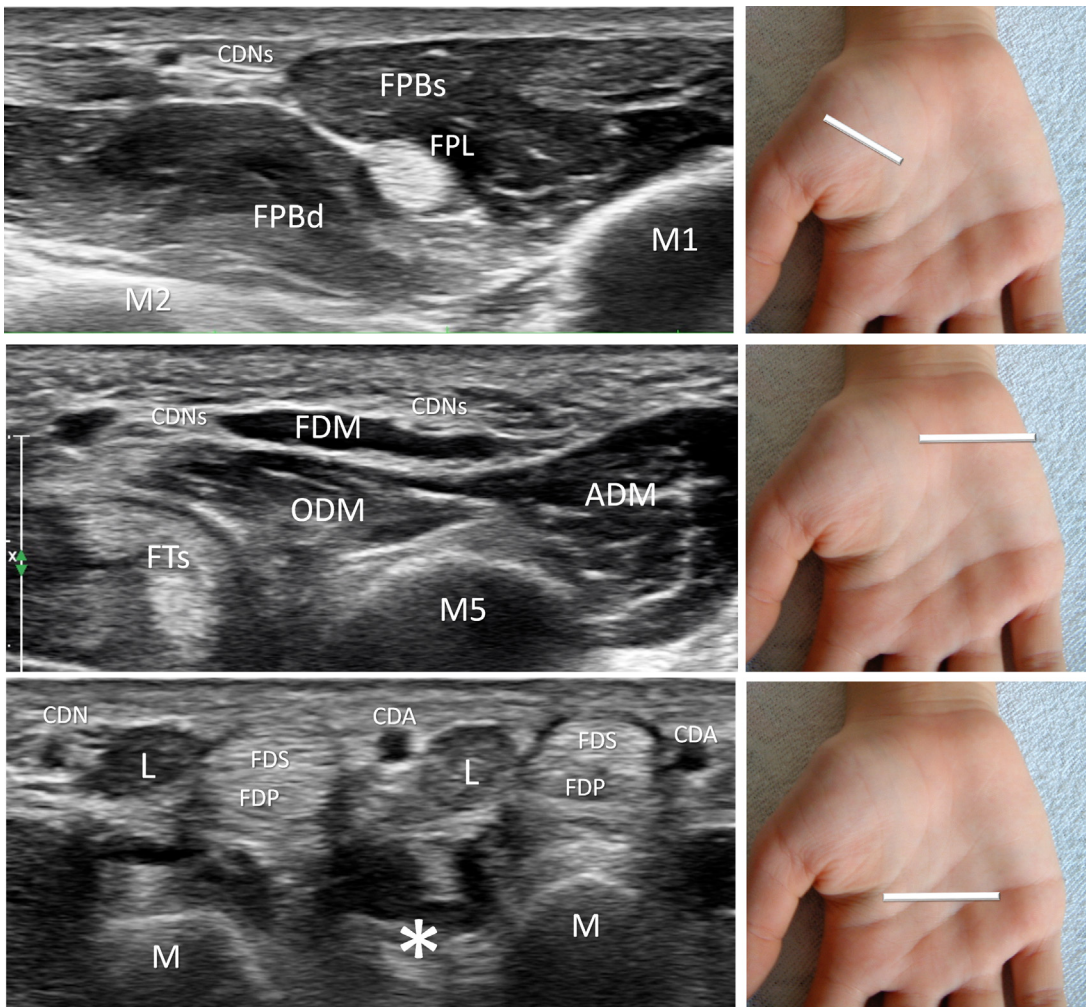
Fig. 19. At the thenar side of the palm, the most lateral flexor tendon is the FPL tendon. This tendon courses between the FPBs and FPBd heads of the FPBm. In the middle palm, the axial view displays the FDS and FDP. On each side of the tendons are located the common digital arteries and nerves and the lumbrical muscles. More deeply, the interosseous muscles (*asterisk*) are seen filling the space between the metacarpals. At the hypothenar side of the palm are situated the adductor digiti minimi (ADM), flexor digiti minimi (FDM), and opponent digiti minimi (ODM) muscles. CDA, common digital artery; CDN, common digital nerve; FDP, flexor digitorum profundus; FDS, flexor digitorum superficialis; FPBd, flexor pollicis brevis, deep head; FPBs, flexor pollicis brevis, superficial head; M1 to M5 first to fifth metacarpal.
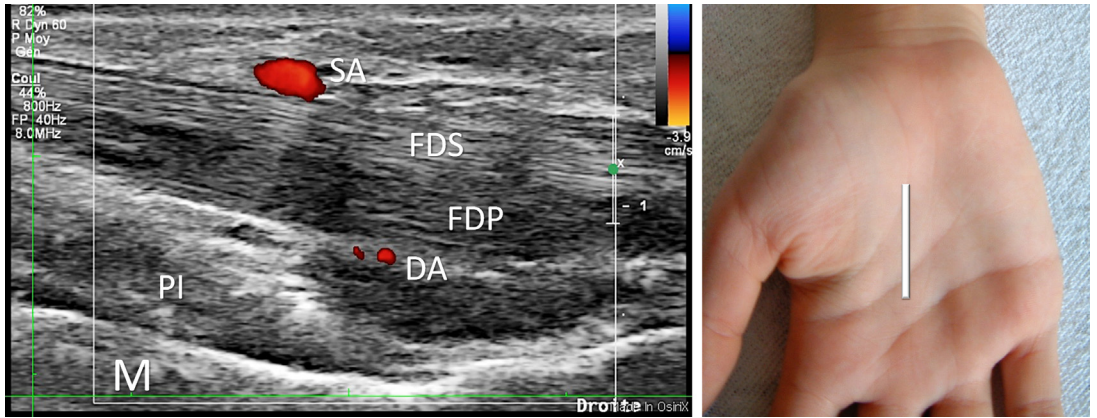
Fig. 20. In the palm, the SA lies superficial to the flexor tendons and is well demonstrated with color Doppler US; the DA is not always clearly identified at the level of the metacarpals and the palmar interosseous muscles. PI, palmar interosseous; SA, superficial arterial arch.
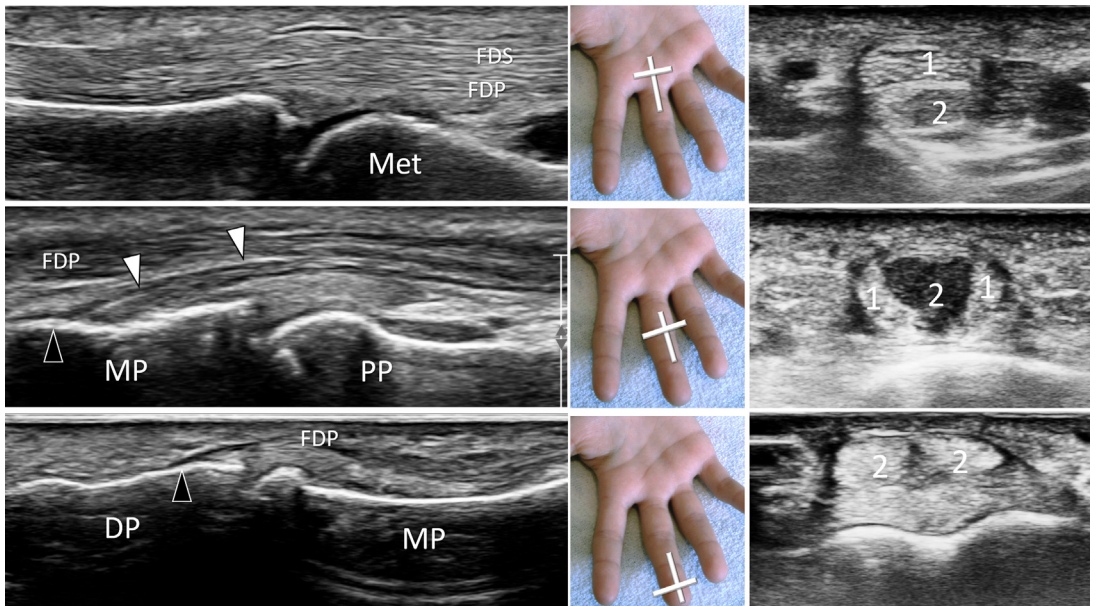

Fig. 21. In the fingers, the FDP and FDS tendons run in the fibrous digital sheath delimited by the volar aspect of the phalangeal cortex and the digital pulleys. When the FDS enters the digital sheath, it splits into 2 tendons (1) to surround the FDP (2). Then, the FDS inserts into the middle phalanx (*white arrowheads*) and the FDP continues toward the distal phalanx and inserts into its base (*black arrowhead*).
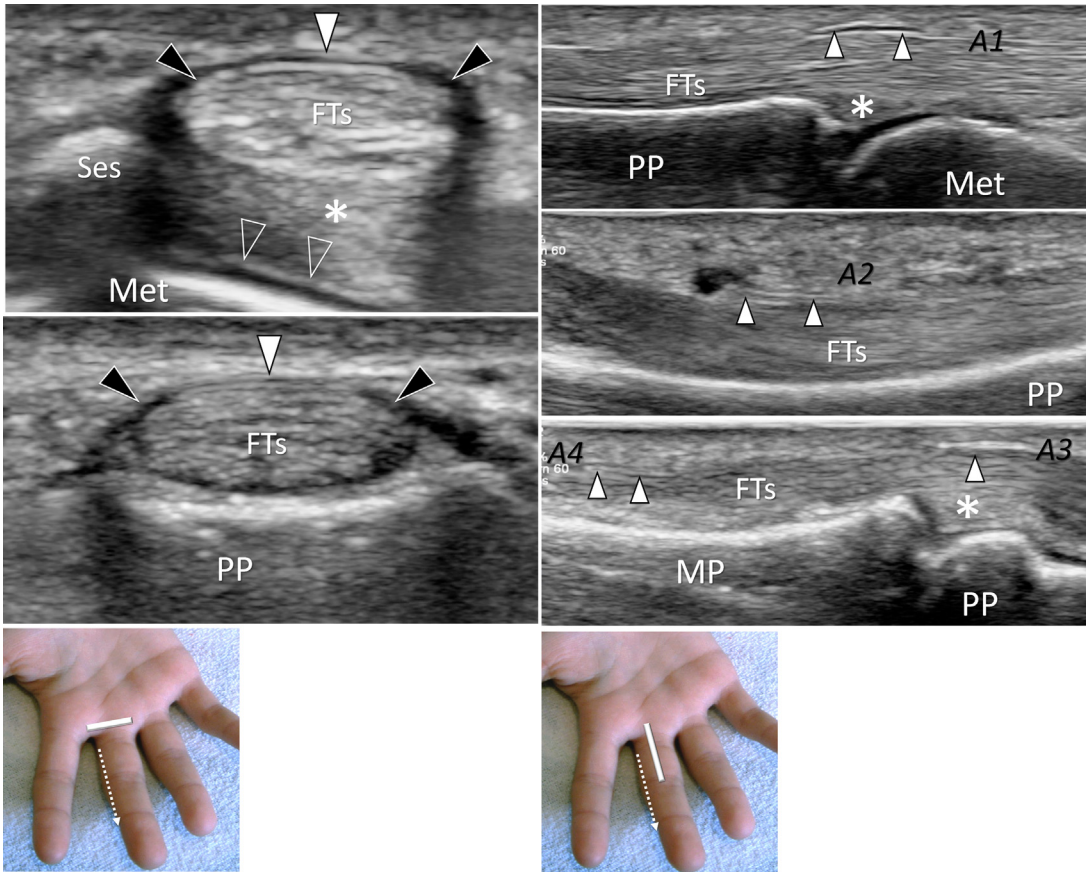
Fig. 22. Normal annular pulleys are less than 1 mm thick. The pulleys are usually hyperechoic when perpendicular to the US beam (*white arrowheads*) and hypoechoic laterally (*black arrowheads*). Dynamic scanning during flexion and extension of the finger illustrates the stationary pulley system from the underlying gliding tendons. Palmar plates (*asterisk*) lie between the FTs and the metacarpal and phalangeal heads. A palmar plate appears normally as a hyperechoic structure, with a rectangular shape on the axial view (see also Fig. 23). The articular cartilage (*white empty arrowheads*) is seen as a fine and regular hypoechoic curved line covering the hyperechoic subchondral bone. A sesamoid is observed as a bright rounded structure with a posterior acoustic shadow at the level of the metacarpophalangeal joint. A1 to A4, first to fourth annular pulley; FTs, flexor tendons; Ses, sesamoid.
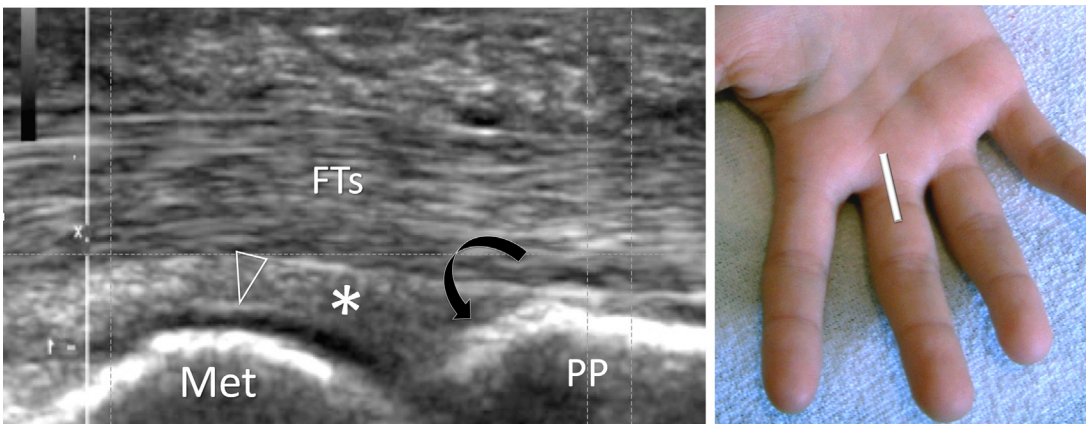

Fig. 23. In the longitudinal view, the palmar plate appears as a triangular hyperechoic structure (*asterisk*), inserting into the base of the phalanx (*curved arrow*) and pointing cranially. The articular cartilage (*white empty arrowhead*) is clearly visible.
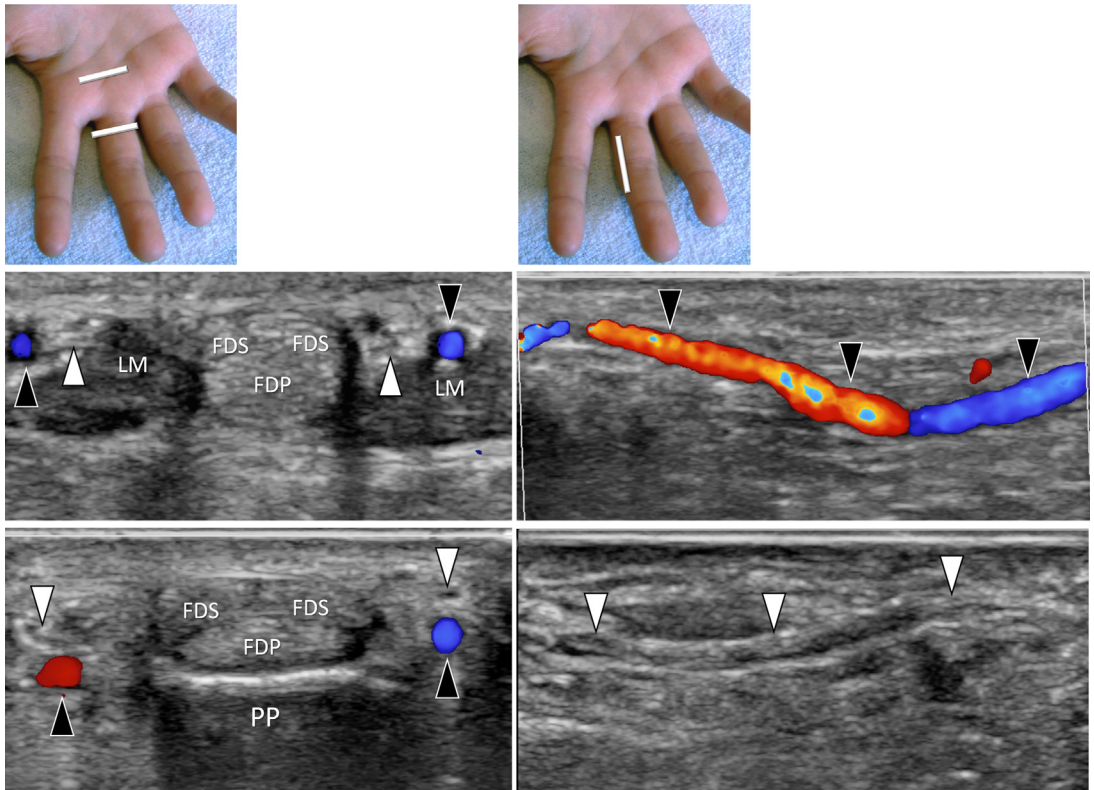
Fig. 24. Digital arteries and nerves run alongside the FDS and FDP tendons, close to the lumbrical muscles. Arteries, usually smaller than the adjacent veins, are better identified with color Doppler US (*black arrowheads*). Nerves (*white arrowheads*) are recognizable by their fascicular appearance. LM, lumbrical muscle.
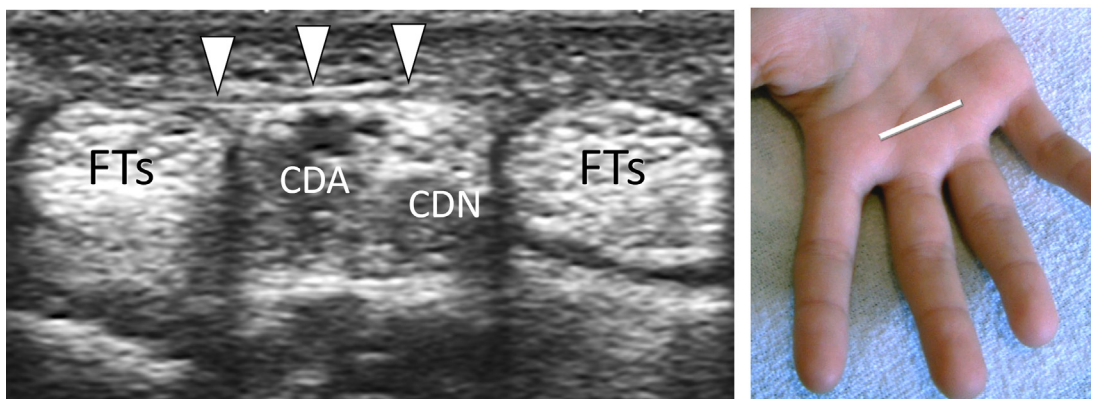

Fig. 25. The palmar aponeurosis is a superficial thin structure (*arrowheads*) that covers the FTs, common digital arteries, and common digital nerves of the palm.

similarly. Normal typical images are presented together with inserts indicating the position or the course of the transducer.

Wrist (**Figs. 1–16**).

Hand (**Figs. 17–25**).

CLINICS CARE POINTS

- Using high-quality equipment (high-frequency linear array transducers ranging from 10 to 15 MHz; adapted size and shape of the probe, like a hockey-stick probe; Doppler imaging; compound imaging; extended field-of-view imaging; steering-based imaging; 3-dimensional imaging; elastography; contrast media; and DICOM capacities for static and dynamic recording)
- Standardization of US examination technique, including first examination on the short axis and then on the long axis plane, dynamic evaluation, and correct focusing.
- Appropriateness of US indications, pertinent clinical information, and patient's history.
- Accurate interpretation of the images and correlation of the US findings with clinical data
- Use of x-rays when superficial cortical outgrowths or ingrowths are suspected

DISCLOSURES OF CONFLICTS OF INTEREST

V. Créteur disclosed no relevant relationships. A. Madani disclosed no relevant relationships. S. Bianchi disclosed no relevant relationships.

REFERENCES

1. Bianchi S, Martinoli C, Sureda D, et al. Ultrasound of the hand. Eur J Ultrasound 2001;14:29–34.
2. Créteur V, Peetrons P. Ultrasonography of the wrist and the hand. J Radiol 2000;81:346–52.
3. Lee JC, Healy JC. Normal sonographic anatomy of the wrist and hand. Radiographics 2005;25:1577–90.
4. Bianchi S, Martinoli C, Abdelwahab F. High-frequency ultrasound examination of the wrist and hand. Skeletal Radiol 1999;28:121–9.
5. Chiavaras MM, Jacobson JA, Yablon CM, et al. Pitfalls in wrist and hand ultrasound. AJR Am J Roentgenol 2014;203:531–40.
6. Catalano O, Roldán FA, Varelli C, et al. Skin cancer: findings and role of high-resolution ultrasound. J Ultrasound 2019;22:423–31.
7. Morvan G, Brasseur J-L, Sans N. Superficial US of superficial bones. J Radiol 2005;86:1892–903.
8. Créteur V, Borens B, Bouchaibi SE, et al. Osteolytic femoral lesion detected by sonography in a case of light chain deposition disease. J Clin Ultrasound 2014;42:444–8.
9. Bianchi S. Ultrasound and bone: a pictorial review. J Ultrasound 2020;23(3):227–57.
10. Peetrons P. Ultrasound of muscles. Eur Radiol 2002; 12:35–43.
11. Martinoli C, Bianchi S, Dahmane M, et al. Ultrasound of tendons and nerves. Eur Radiol 2002; 12:44–55.
12. Gitto S, Draghi F. Normal sonographic anatomy of the wrist with emphasis on assessment of tendons, nerves, and ligaments. J Ultrasound Med 2016;35: 1081–94.
13. Moraux A, Vandenbossche L, Demondion X, et al. Anatomical study of the pisotriquetral joint ligaments using ultrasonography. Skeletal Radiol 2012;41:321–8.
14. Créteur V, Bacq C, Widelec J. Sonography of peripheral nerves-first part: upper limb. J Radiol 2004;85:1887–99.
15. Petrover D, Bellity J, Vigan M, et al. Ultrasound imaging of the thenar motor branch of the median nerve: a cadaveric study. Eur Radiol 2017;27: 4883–8.
16. Bianchi S, J-Beaulieu Y, Poletti P-A. Ultrasound of the ulnar-palmar region of the wrist : normal anatomy and anatomic variations. J Ultrasound 2020;23(3): 349–62.
17. Créteur V, Madani A, Gosset N. Apport de l'échographie dans la maladie de Dupuytren. J Radiol 2010; 91:687–91.
18. Draghi F, Gitto S, Bianchi S. Injuries to the collateral ligaments of the metacarpophalangeal and interphalangeal joints. J Ultrasound Med 2018;37(9): 2117–33.
19. Bianchi S, Gitto S, Draghi F. Ultrasound features of trigger finger review of the literature. J Ultrasound Med 2019;38(12):3141–54.
20. Bianchi S, Becciolini M. Ultrasound evaluation of sesamoid fractures of the hand. J Ultrasound Med 2019;38:1913–20.
21. Créteur VM, Durieux PF, Cuylits N. Case 247: Jersey finger of the fifth finger. Radiology 2017;285:683–9.